Mitochondrial Genome Variation Affects Multiple Respiration and Nonrespiration Phenotypes in *Saccharomyces cerevisiae*

Sriram Vijayraghavan,* Stanislav G. Kozmin,*,[1] Pooja K. Strope,*,[2] Daniel A. Skelly,[†,3] Zhenguo Lin,[‡] John Kennell,[‡] Paul M. Magwene,[†] Fred S. Dietrich,* and John H. McCusker*,[4]

*Department of Molecular Genetics and Microbiology, Duke University Medical Center, Durham, North Carolina 27710, [†]Department of Biology, Duke University, Durham, North Carolina 27708, and [‡]Department of Biology, Saint Louis University, Missouri 63103

ORCID ID: 0000-0002-7659-2589 (P.M.M.)

ABSTRACT Mitochondrial genome variation and its effects on phenotypes have been widely analyzed in higher eukaryotes but less so in the model eukaryote *Saccharomyces cerevisiae*. Here, we describe mitochondrial genome variation in 96 diverse *S. cerevisiae* strains and assess associations between mitochondrial genotype and phenotypes as well as nuclear-mitochondrial epistasis. We associate sensitivity to the ATP synthase inhibitor oligomycin with SNPs in the mitochondrially encoded *ATP6* gene. We describe the use of iso-nuclear F1 pairs, the mitochondrial genome equivalent of reciprocal hemizygosity analysis, to identify and analyze mitochondrial genotype-dependent phenotypes. Using iso-nuclear F1 pairs, we analyze the oligomycin phenotype-*ATP6* association and find extensive nuclear-mitochondrial epistasis. Similarly, in iso-nuclear F1 pairs, we identify many additional mitochondrial genotype-dependent respiration phenotypes, for which there was no association in the 96 strains, and again find extensive nuclear-mitochondrial epistasis that likely contributes to the lack of association in the 96 strains. Finally, in iso-nuclear F1 pairs, we identify novel mitochondrial genotype-dependent nonrespiration phenotypes: resistance to cycloheximide, ketoconazole, and copper. We discuss potential mechanisms and the implications of mitochondrial genotype and of nuclear-mitochondrial epistasis effects on respiratory and nonrespiratory quantitative traits.

KEYWORDS *Saccharomyces cerevisiae*; mitochondrial genome variation; phenotypic variation; transgression; nuclear-mitochondrial epistasis; Introgression

MITOCHONDRIAL genome polymorphisms and nuclear-mitochondrial epistasis have been extensively studied in multicellular model organisms (Ballard and Melvin 2010; Joseph *et al.* 2013) and in humans. In humans, polymorphisms in both the maternally inherited mitochondrial genome and the nuclear genome are major sources of drug-induced and inherited mitochondrial diseases (Carelli *et al.* 2003; Thorburn 2004; Dimauro and Davidzon 2005; Taylor and Turnbull 2005; Graziewicz *et al.* 2006; Mancuso *et al.* 2007; Barnhill *et al.* 2012; Schapira 2012; Singh *et al.* 2014; Lodi *et al.* 2015). Relative to its size (16,569 bp; 37 genes), human mitochondrial genome polymorphisms are responsible for a large proportion of these mitochondrial diseases. The large proportion of mitochondrial genotype-dependent human mitochondrial diseases may reflect nuclear-mitochondrial epistasis that arises because all mitochondrially encoded RNAs and proteins form complexes with at least one, and often multiple, nuclearly encoded proteins. Both the human and *Saccharomyces cerevisiae* mitochondrial genomes contain a small subset of the genes required for mitochondrial translation and for respiration and in both species most of

doi: https://doi.org/10.1534/genetics.118.301546
Manuscript received August 28, 2018; accepted for publication November 20, 2018; published Early Online November 29, 2018.
Supplemental material available at Figshare: https://doi.org/10.25386/genetics.7361240.
[1]Present address: Department Molecular and Human Genetics, Baylor College of Medicine, Houston, TX 77030-3411.
[2]Present address: National Center for Biotechnology Information, National Library of Medicine, National Institutes of Health, Bethesda, MD 20892.
[3]Present address: The Jackson Laboratory, Bar Harbor, ME 04609.
[4]Corresponding author: Department of Molecular Genetics and Microbiology, Duke University Medical Center, 3020, Room 239, Jones Bldg., 561 Research Drive, Durham, NC 27710. E-mail: john.mccusker@duke.edu

the 500–1500 member mitochondrial proteome is nuclearly encoded (Steinmetz *et al.* 2002a; Sickmann *et al.* 2003; Perocchi *et al.* 2008; Rhee *et al.* 2013). Thus, *S. cerevisiae* is an excellent model for studies of human mitochondrial and nuclear-mitochondrial gene product functions (Steinmetz *et al.* 2002a; Schwimmer *et al.* 2006; Perocchi *et al.* 2008; Baile and Claypool 2013; Rutter and Hughes 2015), as well as for nuclear-mitochondrial pathogenic polymorphisms (Stumpf and Copeland 2011; Montanari *et al.* 2013; Kabala *et al.* 2014; Lodi *et al.* 2015).

In addition to being a model for mitochondrial and nuclear-mitochondrial gene product functions, *S. cerevisiae* is a well-established model for population and quantitative genetics studies (Liti and Louis 2012; Fay 2013; Strope *et al.* 2015; Peter *et al.* 2018). However, *S. cerevisiae* population and quantitative genetics studies have almost exclusively focused on nuclear genome sequences and phenotypic contributions with relatively few studies considering the phenotypic contributions of mitochondrial genome variation (Codón *et al.* 1995; Dimitrov *et al.* 2009; Edwards *et al.* 2014; Paliwal *et al.* 2014; Wolters *et al.* 2018). We previously described the nuclear genome sequences, phenotypes, and nuclear genotype-phenotype associations in the 100-genomes collection of *S. cerevisiae* strains (Strope *et al.* 2015). In this work, we annotate the mitochondrial genomes of 93 *S. cerevisiae* strains sequenced by Strope *et al.* (2015). In addition, we test for associations of previously determined phenotypes (Strope *et al.* 2015) and novel respiration phenotypes with *S. cerevisiae* mitochondrial genome variation. Finally, we identify mitochondrial genotype-dependent contributions to multiple respiration and nonrespiration phenotypes, as well as extensive nuclear-mitochondrial epistasis.

Materials and Methods

Strains

The *S. cerevisiae* strains listed in Supplemental Material, Table S1 have been deposited in and should be requested from the Fungal Genetics Stock Center (http://www.fgsc.net). For additional descriptions of the sequenced *S. cerevisiae* strains or genetic backgrounds in Table S1, see Strope *et al.* (2015).

Mitochondrial genome assemblies, annotation, and phylogenies

We isolated and sequenced genomic DNA from 93 *S. cerevisiae* strains as described previously (Strope *et al.* 2015). We assembled the mitochondrial genomes from the 93 *S. cerevisiae* strains using the *de novo* assembler ABySS (v.1.3.4), with parameters "k" (the k-mer length), "n" (the minimum number of pairs needed to join contigs), and "c" (the minimum mean k-mer coverage of a unitig) optimized for each strain. Assembly of mitochondrial genomes was carried out using a range of parameters, using ABySS, and also velvet, with the goal of obtaining complete genomes. In most cases, multiple assemblies were combined. In some cases, it was necessary to use an exhaustive assembly algorithm (pondslime) that uses quality scores, to overcome the problems of assembly of highly AT-rich sequences with numerous sequence errors. For the mitochondrial genomes, N50 scores in the 5–15 kb range were generally good. Higher N50 scores often involved chimeric assemblies due to inappropriate joining of AT-rich runs by the nonquality score–based assemblers. Once the mitochondrial genome assemblies were complete, they were checked using Pilon (Broad Institute) as well as checked for paired-end pairing errors, "gene errors" (whether the eight conserved protein-encoding genes and the ribosomal rDNA/transfer RNA (tRNA) encoding genes were all present and intact), and completeness. Completeness was determined using BWA to generate a .sam file for each set of sequences aligned against the genome assembled from it. Sequence reads not aligning were assembled (velvet) and used to determine if pieces of the mitochondrial genomes had been inadvertently left out.

We identified mitochondrial sequences by high read depths relative to single copy nuclear genes and by homology to previously sequenced *Saccharomyces* mitochondrial genomes, genes, and introns. We also used BLAST, ssearch36, LAGAN, EMBOSS tools, and Perl scripts to identify mitochondrial genes and sequence polymorphisms relative to the reference S288c mitochondrial genome. Table files were created with the mitochondrial gene coordinates for each strain. We used the NCBI tool tbl2asn (http://www.ncbi.nlm.nih.gov/genbank/tbl2asn2/) to annotate the mitochondrial genome of each strain.

We used BWA and samtools to estimate the mitochondrial genome copy number of these 93 *S. cerevisiae* strains, which were all grown under the same conditions, by read depths of the mitochondrial *21S* recombinant DNA gene relative to *MDN1*, a single-copy nuclear gene. *21S* was used for estimating mitochondrial depth of coverage because it is by far the largest mitochondrial gene (4438 bp with and 3731 bp without the *SCE1* intron), is found in all mitochondrial genomes, and is conserved. *MDN1* was chosen as the nuclear marker for estimating depth of coverage because it is the largest protein coding gene in the nuclear genome and does not contain repetitive sequences.

The mitochondrial genome sequences of 128 strains in 8 *Saccharomyces* species (Foury *et al.* 1998; Fritsch *et al.* 2014; Strope *et al.* 2015; Leducq *et al.* 2017; Sulo *et al.* 2017) were screened for *ATP6* and *ENS2* gene sequences. Evolutionary histories of these genes were inferred by using the maximum likelihood (ML) method, using MEGA6 (Tamura *et al.* 2013). For each gene family, we calculated Bayesian information criterion (BIC) scores for 24 different nucleotide substitution models using their sequence alignments in MEGA6 (Tamura *et al.* 2013). The nucleotide substitution model with the lowest BIC scores are considered to describe the substitution pattern the best, which was used in the ML phylogenetic inference. Specifically, the Hasegawa–Kishino–Yano model (Hasegawa *et al.* 1985) was used for *ATP6* and the Tamura 3-parameter model (Tamura 1992)

was used for *ENS2*. Nonuniformity of evolutionary rates among sites were modeled by using a discrete γ-distribution (+G) with five rate categories, and by assuming that a certain fraction of sites were evolutionarily invariable (+I).

Iso-nuclear F1 strain construction

We constructed iso-nuclear (*i.e.*, isogenic nuclear genomes) F1 pairs, the mitochondrial genome equivalent of reciprocal hemizygosity analysis (Steinmetz *et al.* 2002b), to identify mitochondrial genotype-dependent phenotypes and to assess nuclear-mitochondrial epistasis. To construct iso-nuclear F1 pairs, we first used the *MIP1*^{DN}-containing plasmid pLND46 (Dimitrov *et al.* 2009) to eliminate the mitochondrial genome from haploid ρ+ strains (Table S1); for each haploid ρ+ strain, we independently generated two ρ0 derivatives. The complete absence of mitochondrial DNA in ρ0 strains was confirmed by the absence of mitochondrial nucleoids (MacAlpine *et al.* 2000). We crossed each of two independently generated ρ0 haploid strains, from which pLND46 had been lost, with haploid ρ+ strains from different genetic backgrounds to create two independent pairs of iso-nuclear F1 diploids: N1 ρ1 × N2 ρ0 → N1/N2 ρ1 and N1 ρ0 × N2 ρ2 → N1/N2 ρ2. We compared the phenotypes of iso-nuclear F1 diploids to identify mitochondrial genotype-dependent contributions to phenotypes (Figure 1).

Media and phenotypic analysis

We performed high-throughput phenotypic analysis of diploid *S. cerevisiae* strains as described previously (Strope *et al.* 2015). Briefly, we grew strains in 80 μl yeast peptone dextrose (YPD) (1% yeast extract, 2% bacto peptone, 2% dextrose) in 384-well plates at 30° for 48 hr. We arrayed strains by robotic pinning (BM5 robot; S&P Robotics) onto rectangular agar plates (catalog number 78116; Greiner Bio-One), at a density of 1536 spots or colonies per plate. To minimize position and neighbor effects, we arrayed each strain in a 6 × 4 block of colonies, with the eight internal colonies from each 6 × 4 block being used to determine phenotypes. We incubated plates at 30° for 1–4 days, unless otherwise specified, that we digitally imaged at 24-hr intervals using the BM5 robot digital camera. We quantified digital images of colony areas using ImageJ 1.47v (http://imagej.nih.gov/ij/index.html) with a Patch Detector Plus plug-in (University of Graz Microscopy Facility; http://microscopy.uni-graz.at/index.php?item=new1). We used the eight internal colonies from each 6 × 4 block to calculate median colony areas for each strain on experimental and control plates; phenotypes were subsequently quantified using the ratio of colony size under experimental *vs.* control conditions. Iso-nuclear F1 strain pairs were analyzed similarly, except for each being arrayed in 3 × 4 blocks. We also phenotypically analyzed some sets of strains by 10-fold spot dilutions (initial cell density: 10^7 cells/ml) onto control and experimental media to assess phenotypes.

Phenotypes were determined on plate media containing 2% agar. Ethanol, the utilization of which requires respiratory competence, and all inhibitors were added to media after autoclaving. Sensitivity to inhibitors of respiration/mitochondrial functions were determined on yeast peptone ethanol (YPE) (1% yeast extract, 2% bacto peptone, 2% ethanol) and/or SE synthetic ethanol (SE) (0.67% yeast nitrogen base without amino acids, 2% ethanol) plates . Growth at low (15°; up to 7 days incubation) and high (39°; up to 7 days incubation) temperatures (30° Control) was tested on YPD, YPEG (YPE + 2% glycerol), synthetic dextrose (SD) (0.67% yeast nitrogen base without amino acids, 2% dextrose), and SEG (SE + 2% glycerol) plates. Sensitivity to nonrespiration inhibitors (cycloheximide, ketoconazole, copper) was determined on YPD and SD plates. Inhibitors, inhibitor concentrations, media used, inhibitor targets, and mitochondrial genes in which resistance mutations previously have been identified are listed in Table S2.

Genotype-phenotype associations

We tested for associations between nuclear genotypes and respiration/mitochondrial inhibitor phenotypes (Table S3), as described previously (Strope *et al.* 2015). We tested for associations between genotypes at 180 mitochondrial genome sites (Table S4) in 96 *S. cerevisiae* strains and previously determined phenotypes (Strope *et al.* 2015), as well as respiration/mitochondrial inhibitor phenotypes (Table S3). Mitochondrial genotypes in the 96 *S. cerevisiae* mitochondrial genome sequences examined included only variation at biallelic sites with a minor allele frequency of ≥5%.

The program GEMMA version 0.94beta (Zhou and Stephens 2012) was used to conduct association tests. This program takes a linear mixed-model approach to controlling population structure using a relatedness matrix (normally constructed from genotype data using GEMMA). To ensure that this matrix accurately reflected relatedness between strains, we constructed the matrix using 171,345 nuclear and mitochondrial biallelic SNPs with minor allele frequency ≥5% (Strope *et al.* 2015). To establish significance of genotype-phenotype associations, we used a threshold of $P < 4 \times 10^{-7}$, which was used by Strope *et al.* (2015) and corresponds to an approximate Bonferroni correction for association mapping using whole-genome genotypes.

Strain and plasmid availability

All strains listed in Table S1 of this work have been deposited into and are available from the Fungal Genetics Stock Center. All plasmids generated as part of this work have been deposited into and are available from Addgene (http://www.addgene.org/John_McCusker/). The *MIP1*^{DN}-containing plasmid pLND46 (Dimitrov *et al.* 2009) was obtained from, and should be requested from, D. Gottschling (CalicoLabs).

Data availability

All *S. cerevisiae* nuclear and mitochondrial genome sequence data has been previously published and deposited (https://doi.org/10.1101/gr.185538.114); see Table S19 of Strope *et al.* (2015) for GenBank accession and Sequence Read

Archive numbers. Supplemental material available at Figshare: https://doi.org/10.25386/genetics.7361240.

Results

S. cerevisiae mitochondrial genome assemblies, sizes, copy numbers, and gene/intron annotations

We assembled the mitochondrial genomes from 93 *S. cerevisiae* strains (Strope *et al.* 2015). With the likely exception of YJM1242, where read depths suggested that the region encompassing the mitochondrial genes *tM(CAU)Q1-COX2-RF1-tF(GAA)Q-tT(UAG)Q2-tV(UAC)Q-COX3-tM(CAU)Q2* may be duplicated, *S. cerevisiae* mitochondrial genome sizes ranged from 73,450 to 92,176 bp (median = 82,308 bp) (Table S5). With the possible exception of the aforementioned YJM1242, the *S. cerevisiae* mitochondrial genomes had the same gene order as the S288c mitochondrial genome (Foury *et al.* 1998). Mitochondrial genome copy number in the 93 *S. cerevisiae* strains ranged from 11 to 77 copies (median = 24) (Table S5). There was a negative association between mitochondrial genome size and copy number (Pearson's correlation = −0.31; $P = 0.00264$). We annotated mitochondrial genes (*21S*, *15S*, *RPM1*, *VAR1*, *COX1*, *COX2*, *COX3*, *COB*, *ATP6*, *ATP8*, *OLI1*, *RF1*, *ENS2*, and 24 tRNAs) in the 93 *S. cerevisiae* (Strope *et al.* 2015) and the three previously published *S. cerevisiae* mitochondrial genome sequences (Foury *et al.* 1998; Fritsch *et al.* 2014) for SNPs and indels (Table S6). We also annotated introns, the presence of which varied widely between strains and in their contributions to mitochondrial genome sizes (Table S7).

ENS2 and ATP6 genotype-phenotype associations and phylogenies

None of the previously determined 49 phenotypes of the 100-genomes strains (Strope *et al.* 2015), including those requiring respiratory competence [*i.e.*, growth on ethanol/glycerol (15, 30, and 39°; rich and defined media) and sporulation (multiple media; 25 and 30°)], showed mitochondrial genotype associations. Thus, for closer focus on the mitochondrial genome, we determined 14 additional phenotypes on media with ethanol or ethanol plus glycerol as the sole carbon source(s), the utilization of which requires respiratory competence (Table S2 and Table S3). With respect to nuclear genotypes, we found multiple phenotype associations (Table S8), including oligomycin sensitivity with loss-of-function polymorphisms in the general stress response regulator-encoding gene *WHI2*, the analysis of which is described in the Supplemental Material.

For these additional 14 respiration phenotypes, we found two mitochondrial genotype associations, both for sensitivity to the ATP synthase inhibitor oligomycin. First, the presence of *ENS2* sequences associated with oligomycin sensitivity (Table S8). When functional, the mobile *ENS2* gene encodes a site-specific endonuclease that has a 26 bp recognition sequence in the *ATP6* ORF (Nakagawa *et al.* 1992). We annotated *ENS2* (Nakagawa *et al.* 1992) in the 96 *S. cerevisiae* strains for presence/absence and, when present, for full-length, potentially functional *ENS2* ORFs, SNPs, and indels (Table S6). In contrast to the presence/absence association, there was no oligomycin association with full-length, potentially functional *ENS2* ORFs (Table S9).

We searched the mitochondrial genome sequences of seven other *Saccharomyces* species (Leducq *et al.* 2017; Sulo *et al.* 2017) and identified *ens2* sequences in *Saccharomyces arboricola* and *Saccharomyces paradoxus* (Figure 2). Similar to *S. cerevisiae* (Figure 3 and Table S6), *ENS2* was located immediately downstream of *ATP6* in *S. arboricola* (two of two strains) as well as in some *S. paradoxus* (9 of 25) strains; there was evidence of *ENS2* introgression (Figure 1, Figure S1, and Figure S2). We determined the *ENS2* phylogeny and identified *ENS2* group A, group B, group 1399, and group *S. paradoxus*; full-length, potentially functional *ENS2* ORFs were present only in *S. cerevisiae* (Figure 2, Figure S1, and Table S6). There was evidence of *ENS2* introgression (Figure 1 and Figure S1).

Oligomycin phenotype also associated with SNPs in the ORF of the ATP synthase subunit-encoding gene *ATP6* (Table S8). The 753, 763, and 766 bp SNPs in the *ATP6* ORF most highly associated with oligomycin phenotype were in linkage disequilibrium. We annotated the ATP synthase subunit-encoding gene *ATP6* in the 96 *S. cerevisiae* mitochondrial genome sequences and identified six groups (*S. cerevisiae* groups 1–5 and 1399) (Figure 1, Figure S1, Figure S2, and Table S6).

We examined the *ATP6* ORFs of the 96 *S. cerevisiae* strains for the more sensitive Ens2 recognition sequence previously identified in an *ens2*^{0} (*i.e.*, no *ens2* sequences) strain (TCATT CAGGGATATGTGTGGGCTATT) and the less-sensitive Ens2 recognition sequence previously identified in an *ENS2*-containing strain (TTATCCAATCTTATGTTTGACTTATC) (Table S6) (Nakagawa *et al.* 1992). The three *S. cerevisiae ENS2* groups (A, B, and 1399), *ens2* sequence presence/absence, the two classes of Ens2 site-specific endonuclease recognition sequences, and the three most highly oligomycin phenotype-associated SNPs coincided with the six *S. cerevisiae ATP6* groups (Figure 2, Figure S1, Figure S2, and Table S6). Finally, we searched the recently published mitochondrial genome sequences of seven other *Saccharomyces* species (Leducq *et al.* 2017; Sulo *et al.* 2017) for *ATP6* and constructed phylogenies. We identified three *S. paradoxus ATP6* groups (*S. paradoxus* groups 1, 2, and 3). In *S. cerevisiae* and *S. paradoxus*, there was evidence of *ATP6* introgression (Figure 2, Figure S1, and Figure S2).

Mitochondrial genotype-dependent oligomycin and other respiration inhibitor phenotypes in iso-nuclear F1 pairs

We first performed a small-scale (12 genetic backgrounds, 8 iso-nuclear F1 pairs) experiment (Figure 1) to test the effects of *ATP6* SNP genotypes on oligomycin phenotypes. In six of these eight iso-nuclear F1 diploid pairs, *ATP6* SNP genotype had the predicted effect on oligomycin phenotype, either mitochondrial genotype-dependent oligomycin resistance/sensitivity phenotypes ($n = 4$; *ATP6*^{R} *vs.* *ATP6*^{S}) or

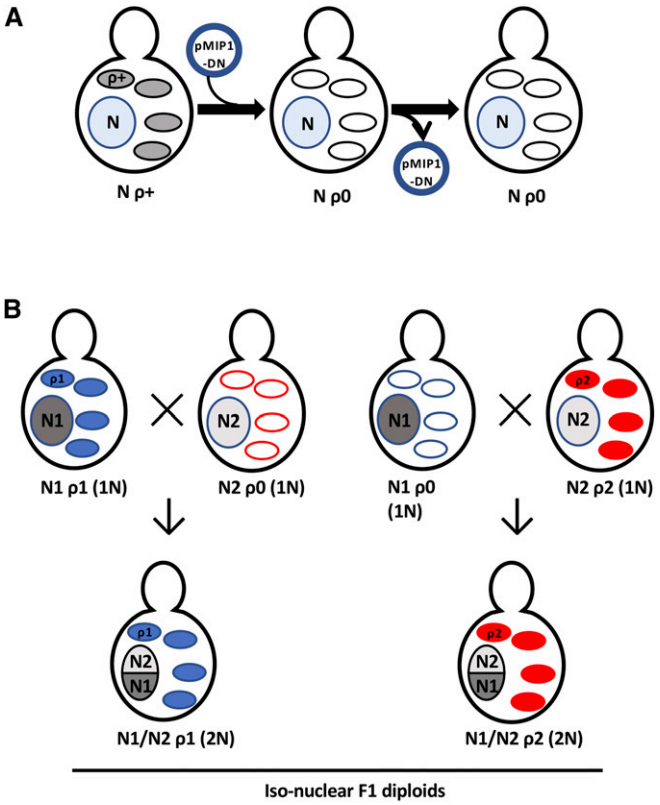

Figure 1 Generation and phenotypic comparison of iso-nuclear F1 diploids. (A) The *MIP1*^{DN}- and centromere-containing plasmid pLND46 (Dimitrov *et al.* 2009) (pMIP1-DN) was introduced into haploid ρ+ strains. *MIP1*^{DN} induction led to the complete loss of the mitochondrial genome, generating ρ0 petites that were then screened for plasmid loss. Nucleus, N-containing blue circle; ovals, parental ρ+ (shaded) and ρ0 (open) mitochondria. (B) Pairwise crosses between haploid ρ+ strains and ρ0 strains of opposite mating types differing in nuclear (N1 *vs.* N2) and mitochondrial (ρ1 *vs.* ρ2) DNA backgrounds generated pairs of iso-nuclear F1 diploids (N1/N2) that carried the parental mitochondrial genomes (ρ1 or ρ2), thus allowing for systematic phenotypic comparison of distinct mitochondrial genomes. Mitochondria: solid blue ovals, ρ1; solid red ovals, ρ2; open ovals, ρ0.

equivalent oligomycin phenotypes (n = 2; *ATP6*^{S} *vs.* *ATP6*^{S}) (Figure 4, Figure S3, Figure S4, and Table S10). However, the remaining two iso-nuclear F1 diploid pairs, both *ATP6*^{S} *vs.* *ATP6*^{S}, nonetheless had mitochondrial genotype-dependent oligomycin resistance/sensitivity phenotypes, consistent with epistasis, with one (YJM1083/YJM627) also being transgressive, *i.e.*, opposite to that predicted by the parental phenotypes (Table S10). We next tested the ability of these eight iso-nuclear F1 diploid pairs to identify mitochondrial genotype-dependent phenotypes for which there were no mitochondrial genotype-phenotype associations. Again, we observed multiple mitochondrial genotype-dependent phenotypes, with some being transgressive (Figure 4, Figures S3–S6, and Table S10).

Because the small-scale experiment was conducted with only 12 genetic backgrounds and 8 iso-nuclear F1 diploid pairs, we expanded our analysis by selecting 14 genetic backgrounds from the 100-genomes strains, haploid derivatives of which we crossed to create a 14 × 14 matrix of diploids: the 14 recreated diploid parent strains plus 91 pairs of iso-nuclear F1 diploids. Similar to the small-scale experiment, we identified iso-nuclear F1 diploid pairs with mitochondrial genotype-dependent oligomycin phenotypes; in some cases, these were consistent with their *ATP6* SNP genotypes (*i.e.*, *ATP6*^{R} *vs.* *ATP6*^{S}) while others were consistent with epistasis (*i.e.*, *ATP6*^{S} *vs.* *ATP6*^{S} and *ATP6*^{R} *vs.* *ATP6*^{R}). Also consistent with epistasis, some *ATP6*^{R} *vs.* *ATP6*^{S} iso-nuclear F1 diploid pairs had equivalent oligomycin phenotypes. Finally, we identified mitochondrial genotype-dependent myxothiazol phenotypes, with many iso-nuclear F1 pairs exhibiting transgression (Table S11).

Mitochondrial genotype-dependent nonrespiration inhibitor phenotypes in iso-nuclear F1 pairs

To test if mitochondrial genotype influenced nonrespiration phenotypes, we determined the spot dilution phenotypes of the aforementioned eight iso-nuclear F1 diploid pairs, and the parent diploids, on SD and/or YPD media, which contained fermentable dextrose as the sole carbon source, for low (15°) and high (39°) temperature growth, as well as for cycloheximide, ketoconazole, and copper resistance. In some of these eight iso-nuclear F1 pairs, we identified mitochondrial genotype-dependent growth temperature, ketoconazole, cycloheximide, and copper resistance phenotypes (Figure 5, Figure 6, and Table S10). The mitochondrial genotype-dependent copper phenotypes in the YJM1083/YJM1418 iso-nuclear F1 pairs were transgressive. Similar to the small-scale experiment, in the 14 × 14 matrix of diploids we identified mitochondrial genotype-dependent phenotypic differences for ketoconazole and cycloheximide resistance; one iso-nuclear F1 pair had transgressive cycloheximide phenotypes (Table S11). Nuclear-mitochondrial genotype epistasis, including transgression, that affects respiratory and nonrespiratory phenotypes is discussed below.

Discussion

The vast diversity in the *S. cerevisiae* mitochondrial genomes in our study population included size, intron content, and copy number variation, as well as SNPs/indels in the 36 core genes [RNA-encoding (n = 27): *21S*, *15S*, *RPM1*, 24 tRNAs; protein-encoding (n = 9): *VAR1*, *COX1*, *COX2*, *COX3*, *COB*, *ATP6*, *ATP8*, *OLI1*, *RF1*]. Some aspects of these *S. cerevisiae* mitochondrial genomes have been previously described (Wolters *et al.* 2015; Peris *et al.* 2017; Repar and Warnecke 2017). Therefore, we focus this discussion on the novel *ENS2* and *ATP6* genotype-oligomycin phenotype associations; *ENS2* and *ATP6* phylogenies and introgression; Ens2-mediated recombination; the identification and characterization of mitochondrial genotype-dependent phenotypes in iso-nuclear F1 pairs; and nuclear-mitochondrial epistasis, as well as its implications for the analysis of quantitative traits.

ENS2 loss-of-function polymorphisms and oligomycin phenotype

With the exception of some group A and group B *ENS2* *S. cerevisiae* strains, most *ens2* ORFs had loss-of-function

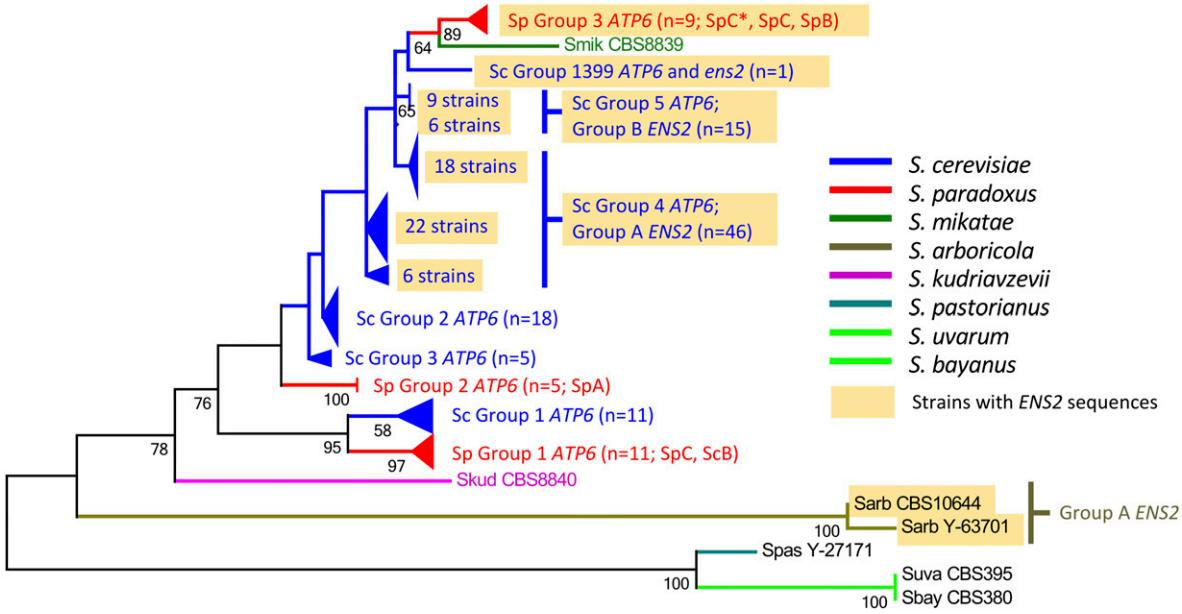

Figure 2 Compressed *ATP6* molecular phylogeny in *Saccharomyces sensu stricto* species. *ATP6* genes were identified from the mitochondrial genome sequences of 128 strains in 8 *S. sensu stricto* species examined, sequences of which were obtained from Strope *et al.* (2015), Leducq *et al.* (2017), Sulo *et al.* (2017). The rate variation model allowed for some sites to be evolutionarily invariable (+I; 84.3517% sites). The tree is drawn to scale, with branch lengths measured in the number of substitutions per site. All codon positions were included for analyses. All positions containing gaps and missing data were eliminated. Light brown shading denotes *ENS2*-containing groups. SpA, SpB, SpC, and SpC* correspond to the *S. paradoxus* population nomenclature of Leducq *et al.* (2017). The three *S. paradoxus ATP6* groups (*S. paradoxus* groups 1 *ATP6 ens2*^{0}, 2 *ATP6 ens2*^{0}, and 3 *ATP6-ens2*) and six *S. cerevisiae ATP6* groups (*S. cerevisiae* group 1 *ATP6 ens2*^{0}, group 2 *ATP6 ens2*^{0}, group 3 *ATP6 ens2*^{0}, group 4 *ATP6-ENS2*, group 5 *ATP6-ENS2*, and group 1399 *ATP6-ens2*) are labeled. For the strains that comprise the three *S. paradoxus ATP6* groups and the six *S. cerevisiae ATP6* groups, see Figure S1, Figure S2, and Table S6.

polymorphisms (Figure S1 and Table S6). What might be the basis for the high frequency of *ens2* loss-of-function polymorphisms? When functional, *ENS2* encodes a site-specific endonuclease and is mobile (Nakagawa *et al.* 1992; Morishima *et al.* 1993). Similarly, some mitochondrial homing introns encode site-specific endonucleases that promote intron mobility. When a site-specific endonuclease-encoding homing intron is fixed, selection for mobility and endonuclease function is lost and, as a result, the homing endonuclease-encoding intron will be lost or accumulate loss-of-function polymorphisms (Burt and Koufopanou 2004). Thus, one hypothesis for the high frequency of *ens2* loss-of-function polymorphisms is lack of selection for Ens2 site-specific endonuclease activity and *ENS2* mobility. A comparison between the mobile *SCE1* intron, which encodes the site-specific endonuclease I-*Sce*I, and the mobile *ENS2* gene in *S. cerevisiae* is informative with respect to the lack of selection hypothesis. Like the homing *SCE1* intron (Table S7), the mobile *ENS2* gene is not fixed in *S. cerevisiae* (Table S6) (*ENS2* is also not fixed in *S. paradoxus* (Figure 1, Figure S1, and Figure S2). However, in contrast to the homing *SCE1* intron that integrates at (and disrupts) the I-*Sce*I recognition sequence in *SCE1*-free *21S* and has no polymorphisms in *S. cerevisiae* (Table S7), *ENS2* does not integrate at (and disrupt) the Ens2 recognition sequence in *ATP6* (*i.e.*, *ENS2* is not homing) and most *ens2* ORFs have inactivating polymorphisms (Table S6). In addition, the less sensitive Ens2 recognition sequence in *ATP6* is not fixed in *S. cerevisiae* (Figure 3 and Table S6). These results argue against the hypothesis that lack of selection for Ens2 site-specific endonuclease activity and *ENS2* mobility is responsible for the high frequency of *ens2* loss-of-function polymorphisms.

A second hypothesis for the high frequency of *ens2* loss-of-function polymorphisms is that there is selection against Ens2 function. Selection against Ens2 function may be a consequence of Ens2-Ssc1 heterodimer formation that might reduce the availability of Ssc1, a nuclearly encoded, mitochondrially localized, essential gene product. Alternatively, selection against functional Ens2 may be a consequence of its site-specific endonuclease activity, which cuts a 26 bp sequence in *ATP6*, and/or the endonuclease activity of functional Ens2-Ssc1 heterodimers, which cut >30 sites in the mitochondrial genome (Morishima *et al.* 1990; Kawasaki *et al.* 1991; Nakagawa *et al.* 1992; Shibata *et al.* 1995; Mizumura *et al.* 1999). That is, functional Ens2 and Ens2-Ssc1 heterodimers presumably introduce deleterious double-stranded DNA breaks in *ENS2*-containing mitochondrial genomes. The less-sensitive Ens2 recognition sequence in functional *ENS2*-containing strains should confer relative resistance to Ens2-mediated double-stranded breaks in *ATP6*. However, the less-sensitive Ens2 recognition sequence would have no effect on Ens2-Ssc1 heterodimer-mediated double-stranded breaks elsewhere in the mitochondrial genome or on reduced availability of

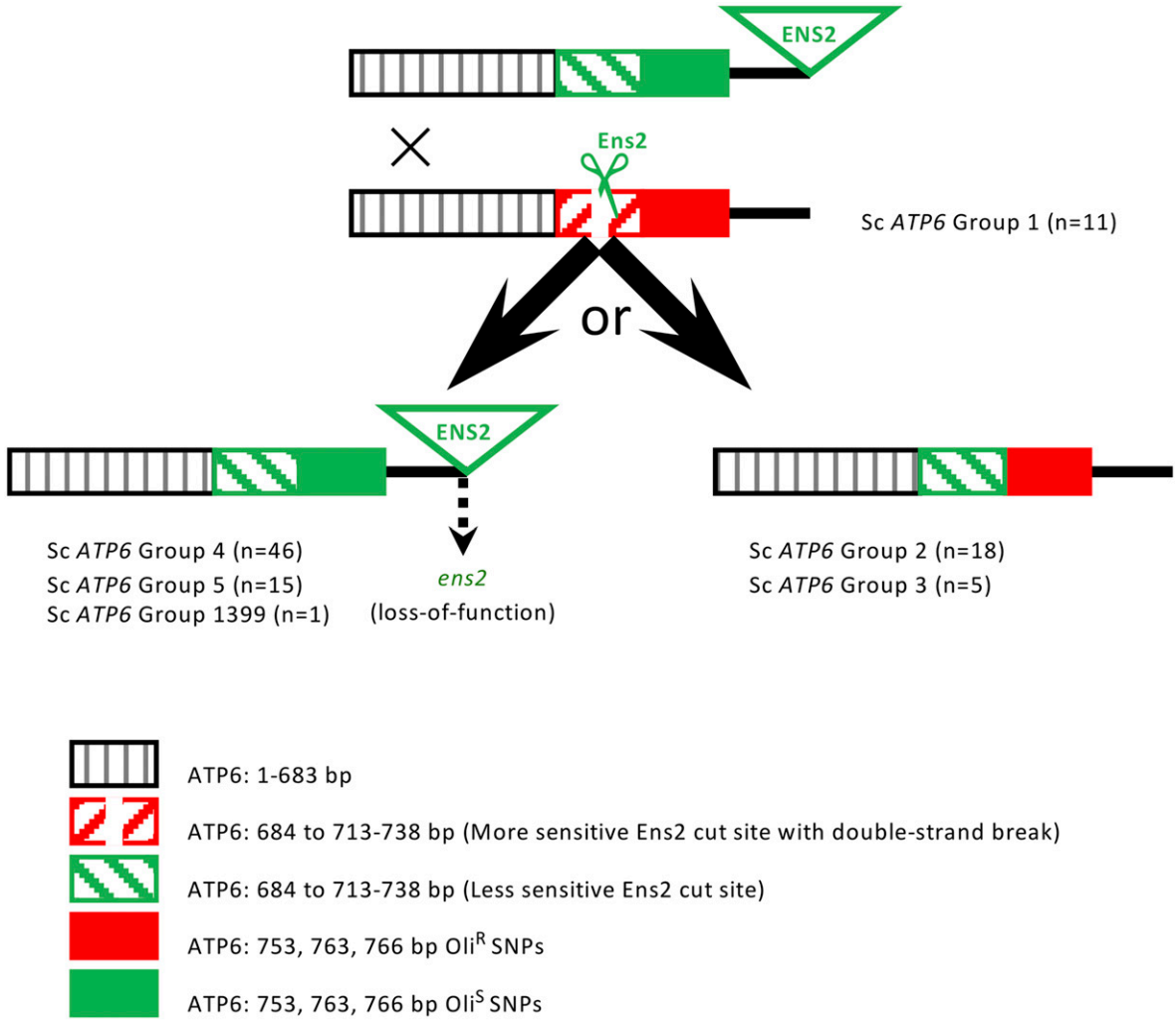

Figure 3 *ATP6-ENS2 vs. ATP6-ens2*^{0} structures and deduced ρ+ *ATP6-ENS2* × ρ+ *ATP6-ens2*^{0} recombination products. Structures of *ATP6-ENS2* [*ATP6*: less-sensitive Ens2 recognition sequence (713–738 bp) and Oli^S SNPs (753, 763, 766 bp); *ENS2* with full-length ORF] and *S. cerevisiae* group 1 *ATP6 ens2*^{0} [*ATP6*: more-sensitive Ens2 recognition sequence (713–738 bp) and Oli^R SNPs (753, 763, 766 bp); no *ENS2* sequences] are shown. The Ens2 recognition sequences, and their relative sensitivities to Ens2, are as previously identified (Nakagawa *et al.* 1992). The distance between the most distal of the Ens2 recognition sequence SNPs (738 bp) and the most proximal of the oligomycin phenotype-associated SNPs (753 bp) is 15 bp. The distance between the most distal of the oligomycin phenotype-associated SNPs (766 bp) and the 5′ end of *ENS2* ORF that, with the exception of YJM1399 (64 bp), is 75–76 bp downstream of the TAA stop codon of the 780 bp *ATP6* ORF, is 89–90 bp. Recombination breakpoints proximal to the Ens2 recognition sequences are proposed to be proximal to the 684 and 693 bp SNPs based on linkage disequilibrium (Table S6). *ATP6* and *ENS2* genotypes and deduced recombination products can be seen in tabular form in Table S6. *ENS2* loss-of-function is proposed to occur postmating. For further details, see *Discussion*.

Ssc1. Only, *ens2* loss-of-function would protect against reduced availability of Ssc1 as well as Ens2- and Ens2-Ssc1–mediated double-stranded DNA breaks in the mitochondrial genome.

Although the basis for the high frequency remains to be determined, the *ens2* loss-of-function polymorphisms were informative with respect to the *ens2* sequence-oligomycin sensitivity association (Table S8). Specifically, consistent with Ens2 function(s) not contributing to oligomycin phenotype, full-length, presumably functional *ENS2* ORFs showed no oligomycin association (Table S9). The basis for the *ENS2* sequence presence-oligomycin sensitivity association, including introgression, is discussed below.

ATP6 phylogeny, ENS2-independent and -dependent introgression of ATP6, Ens2-mediated recombination, and oligomycin phenotype in *S. cerevisiae*

The complex *ATP6* phylogeny showed evidence of both *ENS2*-independent and -dependent introgression of *ATP6*. With respect to *ENS2*-independent *ATP6* introgression, we identified *ATP6 ens2*^{0} groups in *S. cerevisiae* (*S. cerevisiae* group 1, 2, and 3 *ATP6*) and in *S. paradoxus* (*S. paradoxus* group 1 and 2 *ATP6*) (Figure 2 and Figure S2). While directionality cannot be assessed, introgression of *ATP6 ens2*^{0} appears to have occurred more than once between *S. cerevisiae* and *S. paradoxus*. Because of the absence of *ENS2*, these *ATP6 ens2*^{0} introgressions are presumed to be *ENS2*-independent.

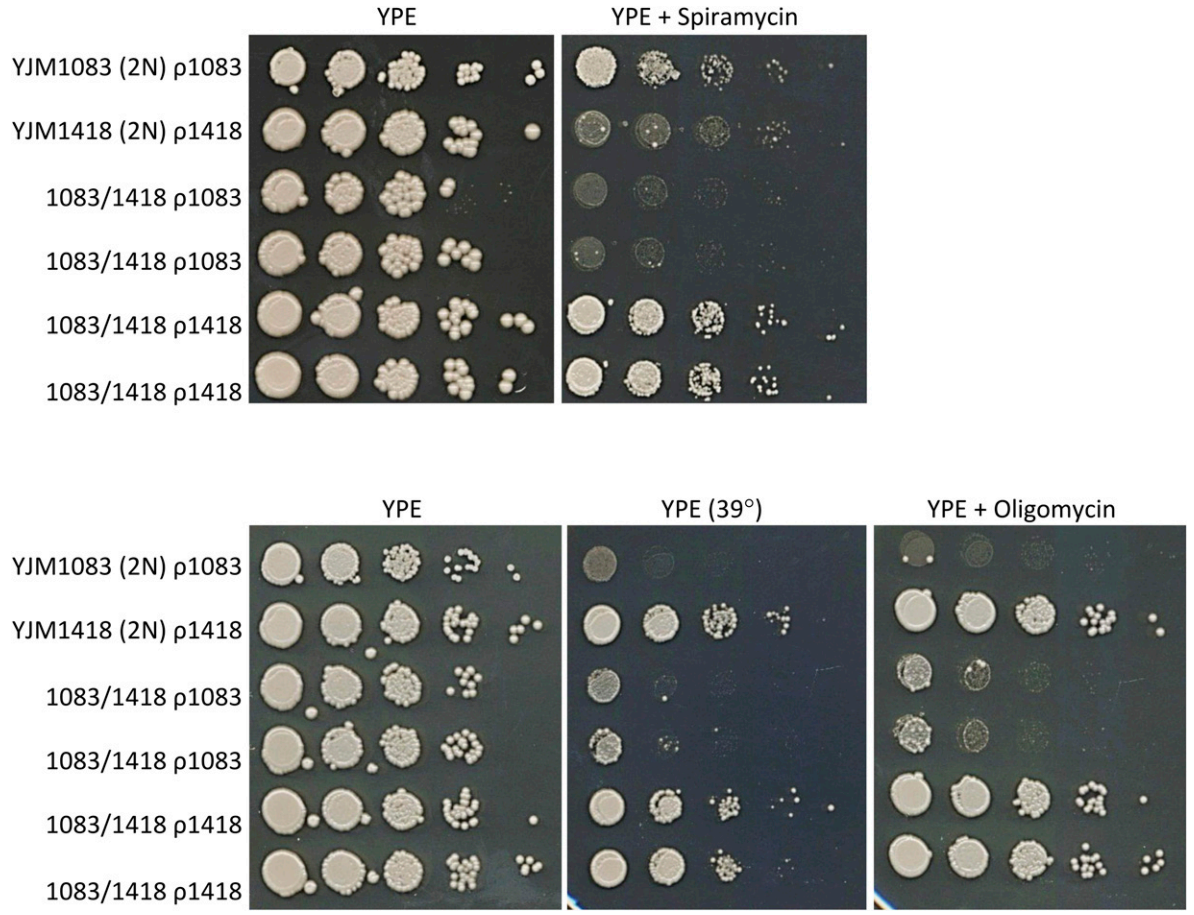

Figure 4 Mitochondrial, genotype-dependent spiramycin, 39°, and oligomycin respiration phenotypes. Spot dilution phenotypes on YPE of parental diploids [YJM1083 ρ1083 (*ATP6*^{S} SNPs) and YJM1418 ρ1418 (*ATP6*^{R} SNPs)] and two independently made iso-nuclear F1 diploid pairs (1083/1418 ρ1083 and 1083/1418 ρ1418). Mitochondrial genotypes are denoted as ρ1083 and ρ1418.

With respect to the hypothesis that cointrogression of *ATP6-ENS2* may be *ENS2*-dependent, we identified *ATP6-ENS2* groups in *S. cerevisiae* (*S. cerevisiae* group 4 *ATP6*/group A *ENS2*; *S. cerevisiae* group 5 *ATP6*/group B *ENS2*; and *S. cerevisiae* group 1399 *ATP6*/group 1399 *ens2*), *S. arboricola* (*S. arboricola ATP6*/group A *ENS2*), and in *S. paradoxus* (*S. paradoxus* group 3 *ATP6*/*S. paradoxus ens2*) (Figure 1 and Figure S1). From the perspective of *ATP6-ENS2* cointrogression, intraspecific *ATP6-ENS2* × *ATP6 ens2*^{0} results in Ens2-dependent, highly biased inheritance of *ENS2* and of a mutation in the *ENS2*-linked *ATP6* (Nakagawa *et al.* 1992; Morishima *et al.* 1993; Shibata *et al.* 1995). The presence of full-length, potentially functional *ENS2* ORFs only in *S. cerevisiae* suggests *ENS2*-mediated introgression from *S. cerevisiae* to *S. arboricola* (*ENS2* only) and to *S. paradoxus* (*ATP6-ENS2*). Consistent with the *ENS2*-mediated introgression hypothesis, with the sole exception of *S. arboricola*, there is strong correspondence between the *ENS2* and *ATP6* phylogenies (Figure 1, Figure S1, and Table S6). One hypothesis for the exception of *S. arboricola* is that *S. cerevisiae ATP6* may be incompatible with *S. arboricola* mitochondrially and/or nuclearly encoded components of ATP synthase.

To assess the hypothesized Ens2-mediated mobility and recombination in *S. cerevisiae*, we examined the Ens2 recognition sequences in *ATP6* [713–738 bp; 11 SNPs that, with the exception of the 721 bp (n = 5; *S. cerevisiae* group 3 *ATP6*) and 723 bp (n = 1; *S. cerevisiae* group 1 *ATP6*] SNPs, were in linkage disequilibrium); two proximal SNPs that were in linkage disequilibrium (684 and 693 bp); the three most highly oligomycin phenotype-associated *ATP6* SNPs that were in linkage disequilibrium (753, 763, and 766 bp); and the presence/absence of *ENS2*. Similar to experimental *ATP6-ENS2* × *ATP6 ens2*^{0} crosses (Nakagawa *et al.* 1992), the data suggests that in *ATP6-ENS2* × *ATP6 ens2*^{0} heteroplasmic zygotes, Ens2-mediated double-stranded DNA breaks at the more sensitive Ens2 recognition sequence of *ATP6 ens2*^{0} (*i.e.*, *S. cerevisiae* group 1 *ATP6*) were repaired and replaced, in most cases, with *ATP6* sequences encompassing the 684 and 693 bp proximal SNPs, the less-sensitive Ens2 recognition sequence, the distal Oli^{S}-associated SNPs, and *ENS2* (Figure 3). That is, in most cases, *ENS2* has driven its movement and, minimally, a 684–766 bp region of *ATP6* into the *S. cerevisiae* population, as exemplified by the *ENS2*-containing *S. cerevisiae* group 4 (n = 46), 5 (n = 15), and YJM1399

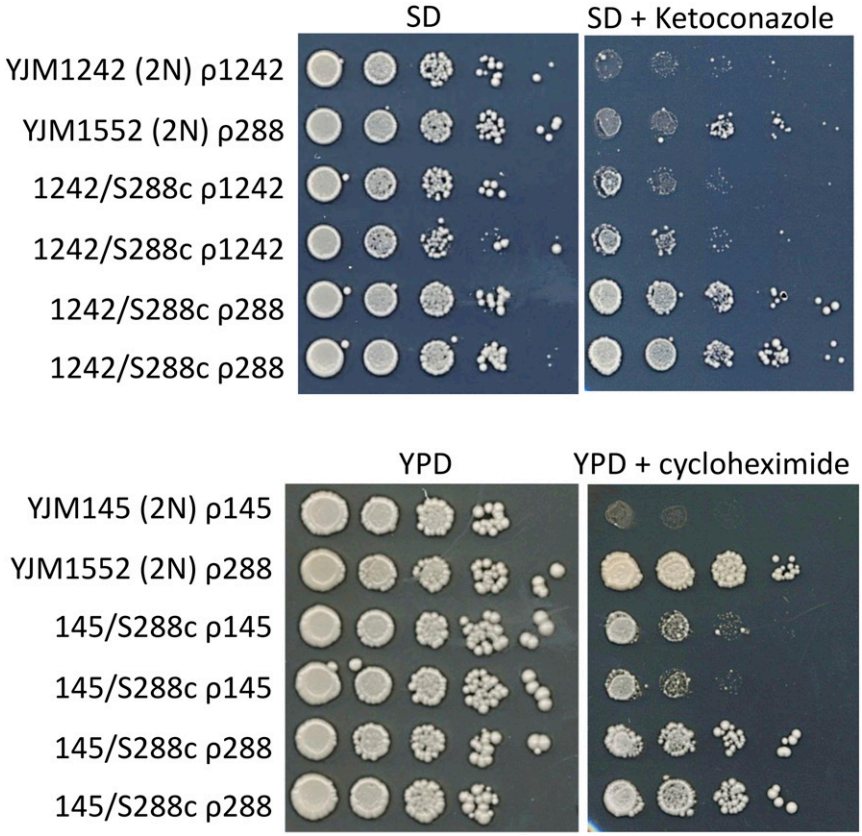

Figure 5 Mitochondrial genotype-dependent, non-respiration ketoconazole and cycloheximide resistance phenotypes. Spot dilution phenotypes on SD (±ketoconazole) and YPD (±cycloheximide) of parental diploids (YJM1242 ρ1242 and YJM1552 ρ288, the diploid YJM1552 is isogenic with S288c; YJM145 ρ145 and YJM1552 ρ288, the diploid YJM145 is isogenic with YJM789) and two independently made iso-nuclear F1 diploid pairs (1242/S288c ρ1242 and 1242/S288c ρ288; 145/S288c ρ145 and 145/S288c ρ288). Mitochondrial genotypes are denoted as ρ1242, ρ288, ρ145, and ρ1418.

(n = 1) *ATP6* strains (note that the T513G oligomycin resistance mutation in *ATP6* that exhibits biased inheritance in experimental *ATP6-ENS2* × *ATP6 ens2*^{0} crosses (Nakagawa *et al.* 1992) is proximal to this minimal 684–766 bp region). However, in the *ens2*^{0} *S. cerevisiae* group 2 *ATP6* (n = 18) and group 3 *ATP6* (n = 5) strains, repair and replacement excluded the Oli^S SNPs and *ENS2* (Figure 3 and Table S6). The oligomycin-resistant phenotypes of these *S. cerevisiae* group 2 and group 3 *ATP6* strains further strengthens the hypothesis that the nonsynonymous 763 and/or 766 bp *ATP6* SNPs contribute to oligomycin phenotype.

The mechanistic basis for the oligomycin phenotype-*ATP6* genotype association remains to be determined. However, oligomycin sensitivity is affected by the level of F0F1 ATP synthase activity (Pagliarani *et al.* 2013). That is, reduced ATP synthase activity results in increased oligomycin sensitivity. Thus, one hypothesis is that the oligomycin sensitivity-*ATP6* genotype association is due to nonsynonymous *ATP6* SNPs that reduce Atp6 stability, the assembly of Atp6 into F0, and/or the assembly of F0 with F1.

Iso-nuclear F1 pairs bypass the limitations of association and illustrate the complexity of mitochondrial genotype-dependent phenotypes

In addition to sample size (n = 96), our identification of mitochondrial genotype-phenotype associations may have been limited by epistasis. To bypass these limitations, we performed more focused experiments to identify and analyze mitochondrial genotype-dependent phenotypes. Previous studies have used *kar1*-mediated mitochondrial genome transfer into novel haploid or homozygous diploid nuclear genetic backgrounds to identify mitochondrial genotype-dependent phenotypes (Codón *et al.* 1995; Dimitrov *et al.* 2009; Edwards *et al.* 2014; Paliwal *et al.* 2014; Spirek *et al.* 2014). However, we did not use *kar1*-mediated mitochondrial genome transfer (Conde and Fink 1976) due to concerns about the potentially confounding cotransfer of 2μ plasmid, amyloid and nonamyloid prions, RNA viruses and satellites, and whole chromosomes (Dutcher 1981; Sigurdson *et al.* 1981; Tartakoff *et al.* 2018). Rather than *kar1*-mediated mitochondrial genome transfer, we used iso-nuclear F1 pairs, in which the parental mitochondrial genotypes are fixed, to identify mitochondrial genotype-dependent phenotypes. Similar to reciprocal hemizygosity analysis in the nuclear genomes of multiply heterozygous F1 diploids (Steinmetz *et al.* 2002b), any difference in the phenotypes of the iso-nuclear F1 diploids must be mitochondrial genotype-dependent (Figure 1). Also, in contrast to *kar1*-mediated mitochondrial genome transfer into novel haploid or homozygous diploid nuclear genetic backgrounds, the nuclear genomes of iso-nuclear F1 diploids closely mimic the nuclear genomes of multiply heterozygous outbred species, such as humans; the multiply heterozygous nuclear genomes of diploid *S. cerevisiae* isolates that occur in nature (McCusker *et al.* 1994; Muller and McCusker 2009; Esberg *et al.* 2011; Magwene *et al.* 2011; Granek *et al.* 2013; Peter *et al.* 2018); and the nuclear

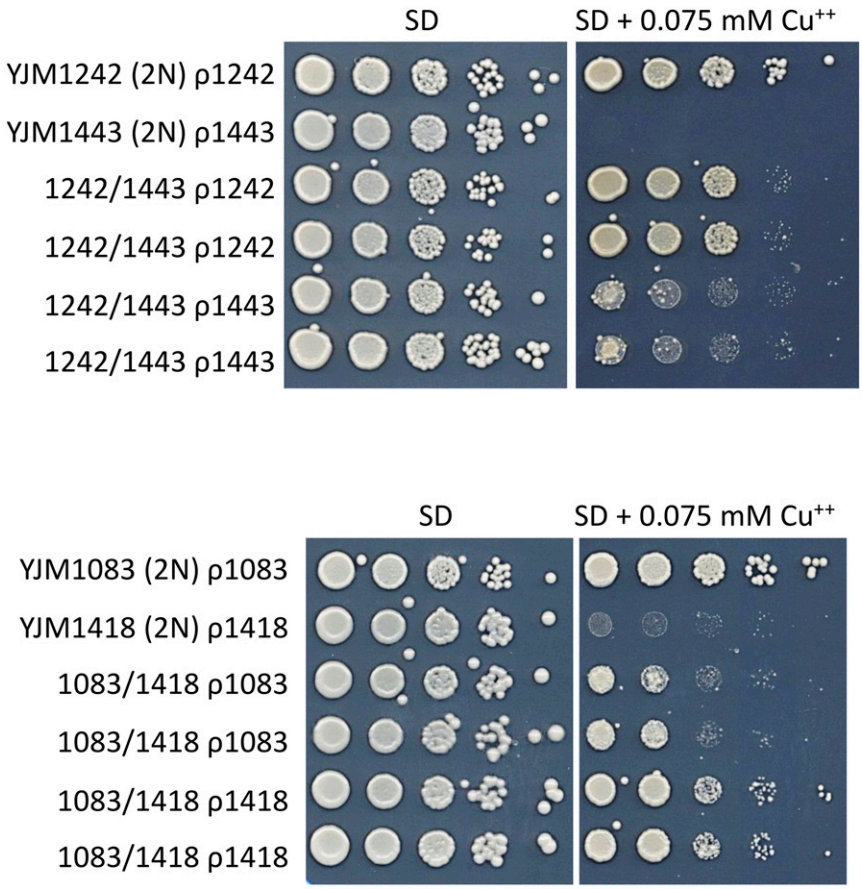

Figure 6 Mitochondrial genotype-dependent, nonrespiration copper resistance phenotypes. Spot dilution phenotypes on SD (±0.075 mM $CuSO_4$) of parental diploids (YJM1242 ρ1242 and YJM1443 ρ1443; YJM1083 ρ1083 and YJM1418 ρ1418) and two independently made, iso-nuclear F1 diploid pairs (1242/1443 ρ1242 and 1242/1443 ρ1443; 1083/1418 ρ1083 and 1083/1418 ρ1418). Mitochondrial genotypes are denoted as ρ1242, ρ1443, ρ1083, and ρ1418. In the 1083/1418 iso-nuclear F1 pairs, mitochondrial genotype-dependent copper resistance is transgressive.

genomes of multiply heterozygous F1 in quantitative genetics studies of *S. cerevisiae* and other species.

Respiration phenotypes

We first analyzed iso-nuclear F1 pairs to experimentally assess the association between oligomycin phenotype and, using the three most highly associated *ATP6* SNPs that are in linkage disequilibrium, *ATP6* genotype (Figure 4, Figure S3, Figure S4, Table S10, and Table S11). Relative to the straightforward oligomycin phenotype-*ATP6* genotype association in our 96 strains, analysis of oligomycin phenotype and *ATP6* genotype in iso-nuclear F1 pairs identified substantial complexity. We feel confident in excluding the other two mitochondrially encoded components of ATP synthase, *OLI1* and *ATP8*, as contributing to the complexity of the oligomycin phenotype in either the 96 parental strains or in iso-nuclear F1 because they each have only one common synonymous SNP and no nonsynonymous SNPs (Table S6). Our iso-nuclear F1 results are consistent with oligomycin phenotype complexity being due to epistatic nuclear-mitochondrial genotype interactions.

We also analyzed iso-nuclear F1 pairs to determine whether other respiration phenotypes, for which there were no mitochondrial genotype associations in our 96 strains, were mitochondrial genotype-dependent. Indeed, we found many iso-nuclear F1 pairs with mitochondrial genotype-dependent respiration inhibitor phenotype(s) (Figure 4, Figure S3–S5, Table S10, and Table S11), some of which exhibited transgression. Broadly, transgression can be viewed as occurring when a quantitative trait locus (in this case, the mitochondrial genome) or gene from a less fit parent increases fitness and, conversely, the locus or gene from the more fit parent decreases fitness. Although typically observed in segregating progeny (Rieseberg *et al.* 1999, 2003; Goulet *et al.* 2017), transgressive alleles have been identified in reciprocally hemizygous F1; for example, alleles of *END3* (Steinmetz *et al.* 2002b; Sinha *et al.* 2006). We hypothesize that extensive nuclear-mitochondrial epistasis, including transgression, is a likely contributor to the lack of other mitochondrial genotype-phenotype associations in the 96 strains.

Nonrespiration phenotypes

Our analysis of iso-nuclear F1 pairs also identified mitochondrial genotype-dependent effects on the nonrespiration growth temperature, cycloheximide, ketoconazole, and copper resistance phenotypes (Figure 5, Figure 6, Table S10, and Table S11). With the exception of high-temperature growth (Paliwal *et al.* 2014; Spirek *et al.* 2014), mitochondrial genotype-dependent effects on these nonrespiration phenotypes are novel. What might be the basis for mitochondrial genotype-dependent effects on nonrespiration phenotypes?

While distinct from the naturally occurring ρ+ mitochondrial genotype variation analyzed in this work, mitochondrial genotype-dependent effects on nonrespiration phenotypes

have been extensively studied in ρ+ *vs.* ρ0 *S. cerevisiae* strains. In ρ0 strains, mitochondrial dysfunction activates a retrograde signaling pathway that affects nuclear gene expression and nonrespiration phenotypes (Butow and Avadhani 2004; Jazwinski 2013; da Cunha *et al.* 2015), including increased cycloheximide resistance in ρ0 strains (Hallstrom and Moye-Rowley 2000; Zhang and Moye-Rowley 2001; Moye-Rowley 2003, 2005; Liu and Butow 2006) (in contrast to cycloheximide, to the best of our knowledge there are no descriptions of retrograde signaling effects on *S. cerevisiae* azole resistance). Thus, one hypothesis is that epistatic nuclear-mitochondrial genotype interactions in some ρ+ iso-nuclear F1 pairs results in mitochondrial dysfunction sufficient to activate a retrograde signaling pathway in one of the iso-nuclear F1 resulting in differential, mitochondrial genotype-dependent, nonrespiration cycloheximide resistance phenotypes.

Alternatively, there is a nonretrograde signaling hypothesis for mitochondrial genotype-dependent cycloheximide resistance. The cytosolic translation inhibitor cycloheximide has been shown to rescue some nuclear mutations that cause mitochondrial dysfunction, possibly by reducing the toxic cytosolic accumulation of nuclearly encoded, mitochondrially targeted proteins (Wang *et al.* 2008; Wang and Chen 2015; Wrobel *et al.* 2015; de Taffin de Tilques *et al.* 2018; Guaragnella *et al.* 2018). Thus, epistatic nuclear-mitochondrial genotype interactions in some ρ+ iso-nuclear F1 pairs may result in cycloheximide-remediable mitochondrial dysfunction in one of the iso-nuclear F1, and consequently, mitochondrial genotype-dependent cycloheximide resistance. Indeed, for one of the iso-nuclear F1 pairs, YJM1450/YJM1479, the mitochondrial genotype-dependent cycloheximide resistance phenotypes were transgressive, consistent with nuclear-mitochondrial epistasis.

We also observed mitochondrial genotype-dependent copper resistance phenotypes in iso-nuclear F1 pairs (Figure 6 and Table S10). To the best of our knowledge, there are no descriptions of retrograde signaling effects on *S. cerevisiae* copper resistance. However, laboratory strains, in which most and possibly all of the work on *S. cerevisiae* ρ+ *vs.* ρ0 and retrograde signaling has been performed, have multiple copies of the copper resistance-conferring, copper metallothionein-encoding gene *CUP1*; for example, the very commonly used S288c and W303 laboratory strains have 14 tandem copies of *CUP1* (Zhao *et al.* 2014). In the 100-genomes strains, the sole and very strong association with copper resistance was *CUP1* copy number, which ranged from one copy to 18 tandem copies (Strope *et al.* 2015). Thus, one hypothesis is that the high *CUP1* copy number in commonly used laboratory strains may be responsible, at least in part, for the lack of previously described ρ+ *vs.* ρ0 or retrograde signaling effects on *S. cerevisiae* copper resistance. Conversely, low *CUP1* copy number may be necessary to detect mitochondrial genotype-dependent copper resistance phenotypes in iso-nuclear F1 pairs. Consistent with the *CUP1* copy number hypothesis, the parent strains of the iso-nuclear F1 pairs that have mitochondrial genotype-dependent copper resistance phenotypes have low *CUP1* copy numbers: YJM1083 (*CUP1*: $n = 3$)/YJM1418 (*CUP1*: $n = 1$) and YJM1242 (*CUP1*: $n = 1$)/YJM1443 (*CUP1*: $n = 1$) (Strope *et al.* 2015).

Although the low *CUP1* copy number hypothesis suggests a reasonable prerequisite for observing mitochondrial genotype-dependent copper resistance, it is not a mechanistic hypothesis. A mechanistic hypothesis for mitochondrial genotype-dependent copper resistance may involve mitochondrially encoded, copper-containing gene product(s) in a mitochondrially localized, copper-dependent enzyme. Of the known copper-containing and copper-dependent enzymes (Festa and Thiele 2011), only the mitochondrially localized cytochrome *c* oxidase contains mitochondrially encoded gene products (Cox1, Cox2, Cox3). Because cytochrome *c* oxidase also contains nuclearly encoded gene products, and requires many additional nuclearly encoded gene products for its synthesis, assembly, and activity, its hypothesized effect on copper resistance may be particularly susceptible to nuclear-mitochondrial epistasis. Indeed, for the YJM1083/YJM1418 iso-nuclear F1 pairs (Figure 6), the mitochondrial genotype-dependent copper resistance phenotypes were transgressive, consistent with nuclear-mitochondrial epistasis. Thus, one hypothesis is that epistatic nuclear-mitochondrial genotype interactions in some iso-nuclear F1 pairs, possibly involving the synthesis, assembly, and/or activity of cytochrome *c* oxidase, may activate a signaling pathway in one of the iso-nuclear F1, resulting in mitochondrial genotype-dependent copper resistance.

In conclusion, naturally occurring mitochondrial genome variation has major phenotypic effects in model systems (Ballard and Melvin 2010; Joseph *et al.* 2013) and in humans (Taylor and Turnbull 2005; Wallace 2010; Schon *et al.* 2012; Dowling 2014). However, with the exception of a relatively small number of studies (Codón *et al.* 1995; Dimitrov *et al.* 2009; Edwards *et al.* 2014; Paliwal *et al.* 2014; Wolters *et al.* 2018), the phenotypic contributions of naturally occurring *S. cerevisiae* mitochondrial genome variation have only infrequently been considered. As we show with iso-nuclear F1 pairs, multiple respiration and nonrespiration phenotypes are strongly influenced by naturally occurring mitochondrial genome variation and by nuclear-mitochondrial epistasis. Even for the presumably straightforward oligomycin phenotype-*ATP6* genotype association, our iso-nuclear F1 analysis showed a high level of complexity. Because of its effect on complex respiration and nonrespiration phenotypes, mitochondrial genotype is likely a major contributor to *S. cerevisiae* quantitative traits. That is, the *S. cerevisiae* mitochondrial genome, which contains 36 core genes (*21S*, *15S*, *RPM1*, *VAR1*, *COX1*, *COX2*, *COX3*, *COB*, *ATP6*, *ATP8*, *OLI1*, *RF1*, 24 tRNAs) and up to 16 mobile and variably present genes (*ENS2* and introns in the *21S*, *COB*, and *COX1* genes), is a 73,450–92,176 bp quantitative trait locus.

In higher eukaryotes and many lower eukaryotes, mitochondrial genome inheritance is uniparental; that is, the mitochondrial genome (ρ) is a fixed, nonrecombinant locus. In contrast, *S. cerevisiae* mitochondrial genome inheritance is biparental (Berger and Yaffe 2000). That is, N1 ρ1 × N2 ρ2

results in N1/N2 heteroplasmic ρ1 + ρ2 zygotes, which tend to produce parental ρ genomes from terminal buds and recombinant ρ genomes from medial buds (Berger and Yaffe 2000). Heteroplasmic N1/N2 ρ1 + ρ2 zygotes produce homoplasmic ρ+ cells via high levels of ρ1×ρ2 recombination (Fritsch *et al.* 2014) and rapid ρ genome segregation (Birky *et al.* 1978; Zinn *et al.* 1987). Recovery of ρ genotypes from heteroplasmic ρ1 + ρ2 zygotes may be biased by prezygotic differences in ρ1 *vs.* ρ2 copy numbers, the frequency of terminal *vs.* medial budding in zygotes, the presence in one of the two parental ρ genomes of *ENS2* and any of the numerous mobile introns, as well as both nuclear-mitochondrial and mitochondrial-mitochondrial epistasis. Thus, N1 ρ1 × N2 ρ2, which has been the standard approach in *S. cerevisiae* quantitative trait studies, yields N1/N2 that are homoplasmic for multiple different mitochondrial genotypes, which negatively affects reproducibility. Fortunately, *S. cerevisiae* mitochondrial genotype can be easily controlled, or fixed, as we have done with iso-nuclear F1 pairs. In addition to allowing the identification and analysis of mitochondrial genotype-dependent phenotypes, controlling *S. cerevisiae* mitochondrial genotype will also enable the identification of mitochondrial genotype-independent *vs.* mitochondrial genotype-dependent quantitative trait genes in the nuclear genome.

Acknowledgments

The authors thank D. Gottschling (CalicoLabs) for the MIP1^{DN}-containing plasmid pLND46, and thank T. Petes, S. Jinks-Robertson, and anonymous reviewers for their comments on and suggestions for this work. This work was supported by National Institutes of Health grant R01 GM098287 awarded to JHM. P.K.S. was supported as a fellow of the Tri-Institutional Molecular Mycology and Pathogenesis Training Program, supported by the National Institutes of Health/National Institute of Allergy and Infectious Diseases (T32 award AI052080-11). National Institutes of Health grant F32 GM110997 supported D.A.S.

Literature Cited

Baile, M. G., and S. M. Claypool, 2013 The power of yeast to model diseases of the powerhouse of the cell. Front. Biosci. (Landmark Ed) 18: 241–278. https://doi.org/10.2741/4098

Ballard, J. W., and R. G. Melvin, 2010 Linking the mitochondrial genotype to the organismal phenotype. Mol. Ecol. 19: 1523–1539. https://doi.org/10.1111/j.1365-294X.2010.04594.x

Barnhill, A. E., M. T. Brewer, and S. A. Carlson, 2012 Adverse effects of antimicrobials via predictable or idiosyncratic inhibition of host mitochondrial components. Antimicrob. Agents Chemother. 56: 4046–4051. https://doi.org/10.1128/AAC.00678-12

Berger, K. H., and M. P. Yaffe, 2000 Mitochondrial DNA inheritance in *Saccharomyces cerevisiae*. Trends Microbiol. 8: 508–513. https://doi.org/10.1016/S0966-842X(00)01862-X

Birky, C. W., R. L. Strausberg, and P. S. Perlman, 1978 Vegetative segregation of mitochondria in yeast: estimating parameters using a random model. Mol. Gen. Genet. 158: 251–261. https://doi.org/10.1007/BF00267196

Burt, A., and V. Koufopanou, 2004 Homing endonuclease genes: the rise and fall and rise again of a selfish element. Curr. Opin. Genet. Dev. 14: 609–615. https://doi.org/10.1016/j.gde.2004.09.010

Butow, R. A., and N. G. Avadhani, 2004 Mitochondrial signaling: the retrograde response. Mol. Cell 14: 1–15. https://doi.org/10.1016/S1097-2765(04)00179-0

Carelli, V., C. Giordano, and G. d'Amati, 2003 Pathogenic expression of homoplasmic mtDNA mutations needs a complex nuclear-mitochondrial interaction. Trends Genet. 19: 257–262. https://doi.org/10.1016/S0168-9525(03)00072-6

Codón, A. C., J. M. Gasent-Ramírez, and T. Benítez, 1995 Factors which affect the frequency of sporulation and tetrad formation in *Saccharomyces cerevisiae* baker's yeasts. Appl. Environ. Microbiol. 61: 630–638 (erratum: Appl. Environ. Microbiol. 61: 1677). http://www.ncbi.nlm.nih.gov/pubmed/7574601

Conde, J., and G. R. Fink, 1976 A mutant of *Saccharomyces cerevisiae* defective for nuclear fusion. Proc. Natl. Acad. U.S.A. 73: 3651–3655. https://doi.org/10.1073/pnas.73.10.3651

da Cunha, F. M., N. Q. Torelli, and A. J. Kowaltowski, 2015 Mitochondrial retrograde signaling: triggers, pathways, and outcomes. Oxid. Med. Cell. Longev. 2015: 482582. https://doi.org/10.1155/2015/482582

de Taffin de Tilques, M., J. P. Lasserre, F. Godard, E. Sardin, M. Bouhier *et al.*, 2018 Decreasing cytosolic translation is beneficial to yeast and human Tafazzin-deficient cells. Microb. Cell 5: 220–232. https://doi.org/10.15698/mic2018.05.629

Dimauro, S., and G. Davidzon, 2005 Mitochondrial DNA and disease. Ann. Med. 37: 222–232. https://doi.org/10.1080/07853890510007368

Dimitrov, L. N., R. B. Brem, L. Kruglyak, and D. E. Gottschling, 2009 Polymorphisms in multiple genes contribute to the spontaneous mitochondrial genome instability of *Saccharomyces cerevisiae* S288C strains. Genetics 183: 365–383. https://doi.org/10.1534/genetics.109.104497

Dowling, D. K., 2014 Evolutionary perspectives on the links between mitochondrial genotype and disease phenotype. Biochim. Biophys. Acta 1840: 1393–1403. https://doi.org/10.1016/j.bbagen.2013.11.013

Dutcher, S. K., 1981 Internuclear transfer of genetic information in *kar1–1/KAR1* heterokaryons in *Saccharomyces cerevisiae*. Mol. Cell. Biol. 1: 245–253. https://doi.org/10.1128/MCB.1.3.245

Edwards, M. D., A. Symbor-Nagrabska, L. Dollard, D. K. Gifford, and G. R. Fink, 2014 Interactions between chromosomal and nonchromosomal elements reveal missing heritability. Proc. Natl. Acad. Sci. USA 111: 7719–7722. https://doi.org/10.1073/pnas.1407126111

Esberg, A., L. A. Muller, and J. H. McCusker, 2011 Genomic structure of and genome-wide recombination in the *Saccharomyces cerevisiae* S288C progenitor isolate EM93. PLoS One 6: e25211. https://doi.org/10.1371/journal.pone.0025211

Fay, J. C., 2013 The molecular basis of phenotypic variation in yeast. Curr. Opin. Genet. Dev. 23: 672–677. https://doi.org/10.1016/j.gde.2013.10.005

Festa, R. A., and D. J. Thiele, 2011 Copper: an essential metal in biology. Curr. Biol. 21: R877–R883. https://doi.org/10.1016/j.cub.2011.09.040

Foury, F., T. Roganti, N. Lecrenier, and B. Purnelle, 1998 The complete sequence of the mitochondrial genome of *Saccharomyces cerevisiae*. FEBS Lett. 440: 325–331. https://doi.org/10.1016/S0014-5793(98)01467-7

Fritsch, E. S., C. D. Chabbert, B. Klaus, and L. M. Steinmetz, 2014 A genome-wide map of mitochondrial DNA recombination in yeast. Genetics 198: 755–771. https://doi.org/10.1534/genetics.114.166637

Goulet, B. E., F. Roda, and R. Hopkins, 2017 Hybridization in plants: old ideas, new techniques. Plant Physiol. 173: 65–78. https://doi.org/10.1104/pp.16.01340

Granek, J. A., D. Murray, Ö. Kayrkçi, and P. M. Magwene, 2013 The genetic architecture of biofilm formation in a clinical isolate of *Saccharomyces cerevisiae*. Genetics 193: 587–600. https://doi.org/10.1534/genetics.112.142067

Graziewicz, M. A., M. J. Longley, and W. C. Copeland, 2006 DNA polymerase gamma in mitochondrial DNA replication and repair. Chem. Rev. 106: 383–405. https://doi.org/10.1021/cr040463d

Guaragnella, N., L. P. Coyne, X. J. Chen, and S. Giannattasio, 2018 Mitochondria-cytosol-nucleus crosstalk: learning from *Saccharomyces cerevisiae*. FEMS Yeast Res. 18: foy088. https://doi.org/10.1093/femsyr/foy088

Hallstrom, T. C., and W. S. Moye-Rowley, 2000 Multiple signals from dysfunctional mitochondria activate the pleiotropic drug resistance pathway in *Saccharomyces cerevisiae*. J. Biol. Chem. 275: 37347–37356. https://doi.org/10.1074/jbc.M007338200

Hasegawa, M., H. Kishino, and T. Yano, 1985 Dating of the human-ape splitting by a molecular clock of mitochondrial DNA. J. Mol. Evol. 22: 160–174. https://doi.org/10.1007/BF02101694

Jazwinski, S. M., 2013 The retrograde response: when mitochondrial quality control is not enough. Biochim. Biophys. Acta 1833: 400–409. https://doi.org/10.1016/j.bbamcr.2012.02.010

Joseph, B., J. A. Corwin, B. Li, S. Atwell, and D. J. Kliebenstein, 2013 Cytoplasmic genetic variation and extensive cytonuclear interactions influence natural variation in the metabolome. eLife 2: e00776. https://doi.org/10.7554/eLife.00776

Kabala, A. M., J. P. Lasserre, S. H. Ackerman, J. P. di Rago, and R. Kucharczyk, 2014 Defining the impact on yeast ATP synthase of two pathogenic human mitochondrial DNA mutations, T9185C and T9191C. Biochimie 100: 200–206. https://doi.org/10.1016/j.biochi.2013.11.024

Kawasaki, K., M. Takahashi, M. Natori, and T. Shibata, 1991 DNA sequence recognition by a eukaryotic sequence-specific endonuclease, Endo.SceI, from *Saccharomyces cerevisiae*. J. Biol. Chem. 266: 5342–5347. http://www.ncbi.nlm.nih.gov/pubmed/2002067

Leducq, J. B., M. Henault, G. Charron, L. Nielly-Thibault, Y. Terrat *et al.*, 2017 Mitochondrial recombination and introgression during speciation by hybridization. Mol. Biol. Evol. 34: 1947–1959. https://doi.org/10.1093/molbev/msx139

Liti, G., and E. J. Louis, 2012 Advances in quantitative trait analysis in yeast. PLoS Genet. 8: e1002912. https://doi.org/10.1371/journal.pgen.1002912

Liu, Z., and R. A. Butow, 2006 Mitochondrial retrograde signaling. Annu. Rev. Genet. 40: 159–185. https://doi.org/10.1146/annurev.genet.40.110405.090613

Lodi, T., C. Dallabona, C. Nolli, P. Goffrini, C. Donnini *et al.*, 2015 DNA polymerase γ and disease: what we have learned from yeast. Front. Genet. 6: 106. https://doi.org/10.3389/fgene.2015.00106

MacAlpine, D. M., P. S. Perlman, and R. A. Butow, 2000 The numbers of individual mitochondrial DNA molecules and mitochondrial DNA nucleoids in yeast are co-regulated by the general amino acid control pathway. EMBO J. 19: 767–775. https://doi.org/10.1093/emboj/19.4.767

Magwene, P., O. Kayikci, J. A. Granek, J. M. Reininga, Z. Scholl *et al.*, 2011 Outcrossing, mitotic recombination, and life-history trade-offs shape genome evolution in *Saccharomyces cerevisiae*. Proc. Natl. Acad. Sci. USA 108: 1987–1992. https://doi.org/10.1073/pnas.1012544108

Mancuso, M., M. Filosto, A. Choub, M. Tentorio, L. Broglio *et al.*, 2007 Mitochondrial DNA-related disorders. Biosci. Rep. 27: 31–37. https://doi.org/10.1007/s10540-007-9035-2

McCusker, J. H., K. V. Clemons, D. A. Stevens, and R. W. Davis, 1994 Genetic characterization of pathogenic *Saccharomyces cerevisiae* isolates. Genetics 136: 1261–1269. http://www.genetics.org/content/136/4/1261.long

Mizumura, H., T. Shibata, and N. Morishima, 1999 Stable association of 70-kDa heat shock protein induces latent multisite specificity of a unisite-specific endonuclease in yeast mitochondria. J. Biol. Chem. 274: 25682–25690. https://doi.org/10.1074/jbc.274.36.25682

Montanari, A., Y. F. Zhou, M. F. D'Orsi, M. Bolotin-Fukuhara, L. Frontali *et al.*, 2013 Analyzing the suppression of respiratory defects in the yeast model of human mitochondrial tRNA diseases. Gene 527: 1–9. https://doi.org/10.1016/j.gene.2013.05.042

Morishima, N., K. Nakagawa, E. Yamamoto, and T. Shibata, 1990 A subunit of yeast site-specific endonuclease SceI is a mitochondrial version of the 70-kDa heat shock protein. J. Biol. Chem. 265: 15189–15197. http://www.ncbi.nlm.nih.gov/pubmed/2203771

Morishima, N., K. Nakagawa, and T. Shibata, 1993 A sequence-specific endonuclease, Endo.SceI, can efficiently induce gene conversion in yeast mitochondria lacking a major exonuclease. Curr. Genet. 23: 537–541. https://doi.org/10.1007/BF00312648

Moye-Rowley, W. S., 2003 Transcriptional control of multidrug resistance in the yeast *Saccharomyces*. Prog. Nucleic Acid Res. Mol. Biol. 73: 251–279. https://doi.org/10.1016/S0079-6603(03)01008-0

Moye-Rowley, W. S., 2005 Retrograde regulation of multidrug resistance in *Saccharomyces cerevisiae*. Gene 354: 15–21. https://doi.org/10.1016/j.gene.2005.03.019

Muller, L. A., and J. H. McCusker, 2009 Microsatellite analysis of genetic diversity among clinical and nonclinical *Saccharomyces cerevisiae* isolates suggests heterozygote advantage in clinical environments. Mol. Ecol. 18: 2779–2786. https://doi.org/10.1111/j.1365-294X.2009.04234.x

Nakagawa, K., N. Morishima, and T. Shibata, 1992 An endonuclease with multiple cutting sites, Endo.SceI, initiates genetic recombination at its cutting site in yeast mitochondria. EMBO J. 11: 2707–2715. https://doi.org/10.1002/j.1460-2075.1992.tb05336.x

Pagliarani, A., S. Nesci, and V. Ventrella, 2013 Modifiers of the oligomycin sensitivity of the mitochondrial F1F0-ATPase. Mitochondrion 13: 312–319. https://doi.org/10.1016/j.mito.2013.04.005

Paliwal, S., A. C. Fiumera, and H. L. Fiumera, 2014 Mitochondrial-nuclear epistasis contributes to phenotypic variation and coadaptation in natural isolates of *Saccharomyces cerevisiae*. Genetics 198: 1251–1265. https://doi.org/10.1534/genetics.114.168575

Peris, D., A. Arias, S. Orlić, C. Belloch, L. Péréz-Través *et al.*, 2017 Mitochondrial introgression suggests extensive ancestral hybridization events among Saccharomyces species. Mol. Phylogenet. Evol. 108: 49–60. https://doi.org/10.1016/j.ympev.2017.02.008

Perocchi, F., E. Mancera, and L. M. Steinmetz, 2008 Systematic screens for human disease genes, from yeast to human and back. Mol. Biosyst. 4: 18–29. https://doi.org/10.1039/B709494A

Peter, J., M. De Chiara, A. Friedrich, J. X. Yue, D. Pflieger *et al.*, 2018 Genome evolution across 1,011 *Saccharomyces cerevisiae* isolates. Nature 556: 339–344. https://doi.org/10.1038/s41586-018-0030-5

Repar, J., and T. Warnecke, 2017 Mobile introns shape the genetic diversity of their host genes. Genetics 205: 1641–1648. https://doi.org/10.1534/genetics.116.199059

Rhee, H. W., P. Zou, N. D. Udeshi, J. D. Martell, V. K. Mootha *et al.*, 2013 Proteomic mapping of mitochondria in living cells via spatially restricted enzymatic tagging. Science 339: 1328–1331. https://doi.org/10.1126/science.1230593

Rieseberg, L. H., M. A. Archer, and R. K. Wayne, 1999 Transgressive segregation, adaptation and speciation. Heredity 83: 363–372. https://doi.org/10.1038/sj.hdy.6886170

Rieseberg, L. H., A. Widmer, A. M. Arntz, and J. M. Burke, 2003 The genetic architecture necessary for transgressive segregation is common in both natural and domesticated populations. Philos. Trans. R. Soc. Lond. B Biol. Sci. 358: 1141–1147. https://doi.org/10.1098/rstb.2003.1283

Rutter, J., and A. L. Hughes, 2015 Power(2): the power of yeast genetics applied to the powerhouse of the cell. Trends Endocrinol. Metab. 26: 59–68. https://doi.org/10.1016/j.tem.2014.12.002

Schapira, A. H., 2012 Mitochondrial diseases. Lancet 379: 1825–1834. https://doi.org/10.1016/S0140-6736(11)61305-6

Schon, E. A., S. DiMauro, and M. Hirano, 2012 Human mitochondrial DNA: roles of inherited and somatic mutations. Nat. Rev. Genet. 13: 878–890. https://doi.org/10.1038/nrg3275

Schwimmer, C., M. Rak, L. Lefebvre-Legendre, S. Duvezin-Caubet, G. Plane *et al.*, 2006 Yeast models of human mitochondrial diseases: from molecular mechanisms to drug screening. Biotechnol. J. 1: 270–281. https://doi.org/10.1002/biot.200500053

Shibata, T., K. Nakagawa, and N. Morishima, 1995 Multi-site-specific endonucleases and the initiation of homologous genetic recombination in yeast. Adv. Biophys. 31: 77–91. https://doi.org/10.1016/0065-227X(95)99384-2

Sickmann, A., J. Reinders, Y. Wagner, C. Joppich, R. Zahedi *et al.*, 2003 The proteome of *Saccharomyces cerevisiae* mitochondria. Proc. Natl. Acad. Sci. USA 100: 13207–13212. https://doi.org/10.1073/pnas.2135385100

Sigurdson, D. C., M. E. Gaarder, and D. M. Livingston, 1981 Characterization of the transmission during cytoductant formation of the 2 micrometers DNA plasmid from *Saccharomyces*. Mol. Gen. Genet. 183: 59–65. https://doi.org/10.1007/BF00270139

Singh, R., L. Sripada, and R. Singh, 2014 Side effects of antibiotics during bacterial infection: mitochondria, the main target in host cell. Mitochondrion 16: 50–54. https://doi.org/10.1016/j.mito.2013.10.005

Sinha, H., B. P. Nicholson, L. M. Steinmetz, and J. H. McCusker, 2006 Complex genetic interactions in a quantitative trait locus. PLoS Genet. 2: e13. https://doi.org/10.1371/journal.pgen.0020013

Spirek, M., S. Polakova, K. Jatzova, and P. Sulo, 2014 Post-zygotic sterility and cytonuclear compatibility limits in *S. cerevisiae* xenomitochondrial cybrids. Front. Genet. 5: 454. https://doi.org/10.3389/fgene.2014.00454

Steinmetz, L. M., C. Scharfe, A. M. Deutschbauer, D. Mokranjac, Z. S. Herman *et al.*, 2002a Systematic screen for human disease genes in yeast. Nat. Genet. 31: 400–404. http://www.ncbi.nlm.nih.gov/pubmed/12134146

Steinmetz, L. M., H. Sinha, D. R. Richards, J. I. Spiegelman, P. J. Oefner *et al.*, 2002b Dissecting the architecture of a quantitative trait locus in yeast. Nature 416: 326–330. https://doi.org/10.1038/416326a

Strope, P. K., D. A. Skelly, S. G. Kozmin, G. Mahadevan, E. A. Stone *et al.*, 2015 The 100-genomes strains, an *S. cerevisiae* resource that illuminates its natural phenotypic and genotypic variation and emergence as an opportunistic pathogen. Genome Res. 25: 762–774. https://doi.org/10.1101/gr.185538.114

Stumpf, J. D., and W. C. Copeland, 2011 Mitochondrial DNA replication and disease: insights from DNA polymerase gamma mutations. Cell. Mol. Life Sci. 68: 219–233. https://doi.org/10.1007/s00018-010-0530-4

Sulo, P., D. Szaboova, P. Bielik, S. Polakova, K. Soltys *et al.*, 2017 The evolutionary history of Saccharomyces species inferred from completed mitochondrial genomes and revision in the 'yeast mitochondrial genetic code'. DNA Res. 24: 571–583. https://doi.org/10.1093/dnares/dsx026

Tamura, K., 1992 Estimation of the number of nucleotide substitutions when there are strong transition-transversion and G+C-content biases. Mol. Biol. Evol. 9: 678–687. https://doi.org/10.1093/oxfordjournals.molbev.a040752

Tamura, K., G. Stecher, D. Peterson, A. Filipski, and S. Kumar, 2013 MEGA6: molecular evolutionary genetics analysis version 6.0. Mol. Biol. Evol. 30: 2725–2729. https://doi.org/10.1093/molbev/mst197

Tartakoff, A. M., D. Dulce, and E. Landis, 2018 Delayed encounter of parental genomes can lead to aneuploidy in *Saccharomyces cerevisiae*. Genetics 208: 139–151. https://doi.org/10.1534/genetics.117.300289

Taylor, R. W., and D. M. Turnbull, 2005 Mitochondrial DNA mutations in human disease. Nat. Rev. Genet. 6: 389–402. https://doi.org/10.1038/nrg1606

Thorburn, D. R., 2004 Mitochondrial disorders: prevalence, myths and advances. J. Inherit. Metab. Dis. 27: 349–362. https://doi.org/10.1023/B:BOLI.0000031098.41409.55

Wallace, D. C., 2010 Mitochondrial DNA mutations in disease and aging. Environ. Mol. Mutagen. 51: 440–450. https://doi.org/10.1002/em.20586

Wang, X., and X. J. Chen, 2015 A cytosolic network suppressing mitochondria-mediated proteostatic stress and cell death. Nature 524: 481–484. https://doi.org/10.1038/nature14859

Wang, X., X. Zuo, B. Kucejova, and X. J. Chen, 2008 Reduced cytosolic protein synthesis suppresses mitochondrial degeneration. Nat. Cell Biol. 10: 1090–1097. https://doi.org/10.1038/ncb1769

Wolters, J. F., K. Chiu, and H. L. Fiumera, 2015 Population structure of mitochondrial genomes in *Saccharomyces cerevisiae*. BMC Genomics 16: 451. https://doi.org/10.1186/s12864-015-1664-4

Wolters, J. F., G. Charron, A. Gaspary, C. R. Landry, A. C. Fiumera *et al.*, 2018 Mitochondrial recombination reveals mito-mito epistasis in yeast. Genetics 209: 307–319. https://doi.org/10.1534/genetics.117.300660

Wrobel, L., U. Topf, P. Bragoszewski, S. Wiese, M. E. Sztolsztener *et al.*, 2015 Mistargeted mitochondrial proteins activate a proteostatic response in the cytosol. Nature 524: 485–488. https://doi.org/10.1038/nature14951

Zhang, X., and W. S. Moye-Rowley, 2001 *Saccharomyces cerevisiae* multidrug resistance gene expression inversely correlates with the status of the F(0) component of the mitochondrial ATPase. J. Biol. Chem. 276: 47844–47852. https://doi.org/10.1074/jbc.M106285200

Zhao, Y., P. K. Strope, S. G. Kozmin, J. H. McCusker, F. S. Dietrich *et al.*, 2014 Structures of naturally evolved CUP1 tandem arrays in yeast indicate that these arrays are generated by unequal nonhomologous recombination. *G3 (Bethesda)* 4: 2259–2269. https://doi.org/10.1534/g3.114.012922

Zhou, X., and M. Stephens, 2012 Genome-wide efficient mixed-model analysis for association studies. Nat. Genet. 44: 821–824. https://doi.org/10.1038/ng.2310

Zinn, A. R., J. K. Pohlman, P. S. Perlman, and R. A. Butow, 1987 Kinetic and segregational analysis of mitochondrial DNA recombination in yeast. Plasmid 17: 248–256. https://doi.org/10.1016/0147-619X(87)90033-3

Communicating editor: L. Steinmetz